Contents lists available at ScienceDirect

Biochemistry and Biophysics Reports

Selective induction of targeted cell death and elimination by near-infrared femtosecond laser ablation

Kazunori Okano [a,b,*], Chung-Han Wang [a], Zhen-Yi Hong [a,b], Yoichiroh Hosokawa [b], Ian Liau [a,c,**]

[a] Department of Applied Chemistry and Institute of Molecular Science, National Chiao Tung University, Hsinchu 300, Taiwan
[b] Division of Materials Science, Nara Institute of Science and Technology, Ikoma 630-0192, Japan
[c] Department of Biological Science and Technology, National Chiao Tung University, Hsinchu 300, Taiwan

ABSTRACT

The techniques for inducing the death of specific cells in tissue has attracted attention as new methodologies for studying cell function and tissue regeneration. In this study, we show that a sequential process of targeted cell death and removal can be triggered by short-term exposure of near-infrared femtosecond laser pulses. Kinetic analysis of the intracellular accumulation of trypan blue and the assay of caspase activity revealed that femtosecond laser pulses induced immediate disturbance of plasma membrane integrity followed by apoptosis-like cell death. Yet, adjacent cells showed no sign of membrane damage and no increased caspase activity. The laser-exposed cells eventually detached from the substrate after a delay of >54 min while adjacent cells remained intact. On the base of in vitro experiments, we applied the same approach to ablate targeted single cardiac cells of a live zebrafish heart. The ability of inducing targeted cell death with femtosecond laser pulses should find broad applications that benefit from precise cellular manipulation at the level of single cells in vivo and in vitro.

1. Introduction

The spatial and temporal regulation of cell death and degeneration is important of maintaining the normal physiology of cells *in vivo*. Cells *in vivo* are arranged in particular spatial patterns in order to regulate their interactions with adjacent cells and extracellular environments. Besides, cells at designated locations need to degenerate at a given time through programmed death in order to make space for adjacent cells to grow [1–5]. Thus, development of an ability of selectively inducing cell death with high spatial and temporal control may facilitate fundamental research on and advance our understanding of cell-cell or cell-matrix interactions *in vivo*. Toward this end, cryoablation has been applied to induce cell death at the atrioventricular node of a guinea pig and for investigation autonomic regulation of biological pacemakers [6].

The near-infrared (NIR) femtosecond (fs) laser (with a energy ranging from subnano to micro J per pulse) has been applied to ablate biological specimens of various types under physiological conditions. Focusing the laser beam with an objective lens further enables one to modify, stimulate and manipulate biological samples with high spatial precision. For example, NIR fs laser has been utilized to cut protein crystals in aqueous solution [7], to cleave chromosomes [8], to ablate

axons in live *C. elegans* [9], to disrupt organelles [10,11] and cells [8, 12], and to dissect tissues [13]. Besides, it has been applied to fabricate adhesive substrates to pattern cells under a culturing condition, and to control cell migration and cell-cell interactions [14–16]. Furthermore, NIR fs laser pulses have been used to stimulate cells of varied types (HeLa, PC12, P19CL6 and C2C12) and tissue regeneration was studied [17]. Meanwhile, it has been shown that NIR fs laser pulses (single or multiple pulses) of moderate energy (0.1–10 nJ/pulse) can generate transient holes on the plasma membrane of cells, which then allows introducing external macromolecules into living cells [18–21]. Besides, it has also been reported that cell death can be induced with laser ablation [12,22,23]. Despite these pioneering works, the ability of NIR fs laser ablation on the manipulation of cells and related novel applications remain not yet fully explored. Besides, details of the change of cells subject to laser ablation has not been completely revealed yet.

Here we report NIR fs laser ablation of cells *in vitro* and *in vivo*. We particularly imaged the temporal change of the targeted ablated cells and cells adjacent to the ablated cells. We verified that NIR fs laser ablation induced cell death with trypan-blue assay [24], and the cell death exhibited apoptosis-like features based on the caspase assay. Notably, the targeted cells eventually detached from the substrate about

* Corresponding author. Division of Materials Science, Nara Institute of Science and Technology, 8916-5 Takayama, Ikoma, 630-0192, Japan.
** Corresponding author. Department of Biological Science and Technology, National Chiao Tung University, Hsinchu, 300, Taiwan.
E-mail addresses: k-okano@ms.naist.jp, kazunori2015@yandex.com (K. Okano), ianliau@mail.nctu.edu.tw (I. Liau).

1 h post ablation whereas the adjacent cells remained largely intact but migrated slightly towards the open space. These collective results illustrate the ability to selectively induced apoptotic cell death at the level of single cells. On the base of the *in vitro* experiments, we further demonstrated NIR fs laser ablation of targeted cardiac cells in the atrium of larval zebrafish.

We anticipate that our approach should find broad applications in research fields that benefit from precise control of cells at the single-cell level such as developmental biology, regenerative medicine or wound healing.

2. Methods

Ethics approval

All experiments were performed in compliance with the relevant laws and institutional guidelines and have been approved by the Animal Investigation Committee of National Chiao Tung University.

2.1. Preparation of micropatterned domains for cell culturing

Plasma-cleaned glass substrates (Borosilicate, 24 mmφ, 0.12–0.17 mm thickness) were coated with cytophobic copolymer of 2-methacry-loyloxyethylphosphorylcholine (MPC) followed by micropatterning to form cell adhesion domains by NIR fs laser scanning as previously reported [25]. In detail, NIR fs laser (1 kHz, 150 μW) was focused with a water immersion objective (20×, NA. 0.5, Olympus, Tokyo Japan) onto the MPC polymer layere in phosphate-buffered saline (PBS) supplemented with 0.1 mg/ml collagen I. The laser scanning rate was 100 μm/s. The MPC polymer film was ablated at 1 μm intervals to form cytophilic domains (20×200 μm^2).

2.2. Culture of cell lines

Normal HepG2 and recombinant HepG2 line (EGFP was expressed in cytoplasm) were kindly gifted from Prof. K. Hasegawa of Institute for Integrated Cell-Material Sciences, Kyoto University. C2C12 (RCB0978) was obtained from RIKEN Cell Bank (Tsukuba, Japan). All the cell lines were cultured to confluence on cytophilic domains or plain glasses in Dulbecco's Modified Eagle's Medium (low glucose) with fetal bovine serum (FBS, 10%) and antibiotic agents (100 units/ml penicillin, 100 μg/ml streptomycin) under CO_2 (5%) and saturated water vapour at 37 °C.

2.3. Maintenance of zebrafish

Zebrafish strain (*Tg(cmlc2:EGFP;cmlc2:H2AFZmCherry)cy13*) was obtained from Taiwan Zebrafish Core Facility at Academia Sinica (TZCFAS) and was maintained according to standard protocols. The strain expresses EGFP-fused cardiac myosin and mChery-fused cardiac histone. Larvae aged at 4 days post-fertilization (dpf) were employed throughout this work.

2.4. Induction of cardiac arrest in the heart of zebrafish

Nifedipine (ACROS Organics), a blocker of the calcium channel, was employed to stop the heartbeat of larval zebrafish [26]. A stock solution (100 mM) was prepared on dissolving nifedipine in dimethylsulfoxide, and stored at −20 °C until use. The stock solution was then diluted to a final concentration of 100 μM with water through vigorous mixing immediately before experiments. To induce cardiac arrest, larval zebrafish were immersed in the diluted solution of nifedipine until the heart eventually ceased beating completely.

2.5. Laser ablation of cultured cells in vitro or cardiac cells in living zebrafish

Setup for NIR fs laser ablation was constructed with inverted microscopes. The laser beam (Ti:Sapphier, 800 nm, 130 fs, 1 kHz; Spitfire Pro or 80 MHz; Tsunami, Spectra-Physics, Newport, USA) was focused on the sample fixed in the culture dish on an inverted microscope through a water immersion objective (20×, NA. 0.5, Olympus or 63×, NA. 1.2, Leica). The energy of the light through the objective lens was adjusted to arbitrary power by controlling a neutral density filter plate.

For *in vitro* cell ablation experiments on micropatterned domains by single NIR fs laser pulse, the regenerated fs laser system (1 kHz, Spitfire Pro) was employed and single pulses were pickuped by mechanical shutter. In order that we can directly observe the processes of the living cell images on real-time, we used a charge-coupled device (CCD) camera (CV-A55IRE, JAI). The sample was illuminated with white light (λ = 400–750 nm) from a halogen lamp and the transmitted light was detected with the CCD camera. An optical filter (Brightline 750/SP, Semrock) was placed in front of the CCD camera to cut the scattered light of the ablating laser beam, which has transmittance (>90%) only at 380–720 nm. A bright-field image in the area of 635×425 pixels was sequentially captured with the CCD camera and stored in a computer.

The experimental setup for the ablation and imaging of fluorescence cells and zebrafish heart was modified from a confocal microscope (TCS SP5II, Leica). For ablation, the beam of a NIR fs pulsed laser (130 fs, 80 MHz, Tsunami) was introduced to the microscope through the back port, and focused through a water-immersion objective lens (63× , NA. 1.2). Fluorescence images were obserbed by the confocal microscope with excitation lasers of 488 nm and 594 nm.

2.6. Caspase 3/7 assay

The active caspase was detected by CaspaTag™ In Situ Caspase-3/7 Detection Kit (APT423, Chemicon Int., Inc.) that uses fluorescence inhibitor, FAM-DEVD-FMK. The inhibitor covalently binds to reactive cysteine residue of active caspase, thereby the FAM-DEVD moiety retained in cytoplasm, emitting fluorescence (Excitation 594 nm, emission 510–540 nm). Assay was performed in accordance of the kit instruction. All process was *in situ* performed without detaching the cells.

3. Results and discussion

To demonstrate laser ablation of single cells *in vitro*, we first incubated cells (HepG2) in PBS solution containing trypan blue and focused the NIR fs laser to the cytoplasm, avoiding the nucleus, of a selected cell (denoted **a** in the upper panel of Fig. 1A). After ablation, the cell started to accumulate trypan blue and numerous membrane blebs formed. Notably, the cells adjacent to the ablated cell remained largely intact (denoted **b** and **c**, Fig. 1A).

To be quantitative, the temporal transmittance of light at varied positions (denoted **a**−**e**, Fig. 1A) was measured. As shown in Fig. 1B, either the transmittance at the soma (**a**) of the targeted cell or a bleb (**d**) nearby the cell diminished dramatically soon after fs laser ablation, and eventually reached a plateau about 10 min post ablation. In contrast, the transmittance at the adjacent cells only decreased slightly within the temporal window (20 min) of our observation (**b** and **c**, Fig. 1A). The collective results indicate the possibility to induce death of single selected cells while keeping the adjacent cells intact using NIR fs laser ablation.

To provide evidence that the NIR fs laser irradiation induced death specifically at the target cells, we performed experiments on two cell types. First, we applied caspase 3/7 assay on mouse myoblast cells (C2C12). As shown in Fig. 2A, only the cell (red arrow) subject to laser ablation (yellow dot denotes the laser focus) became positive (green fluorescence) within 1 h post ablation whereas the adjacent cells show no sign of increased fluorescence (Fig. 2A). This result indicates the
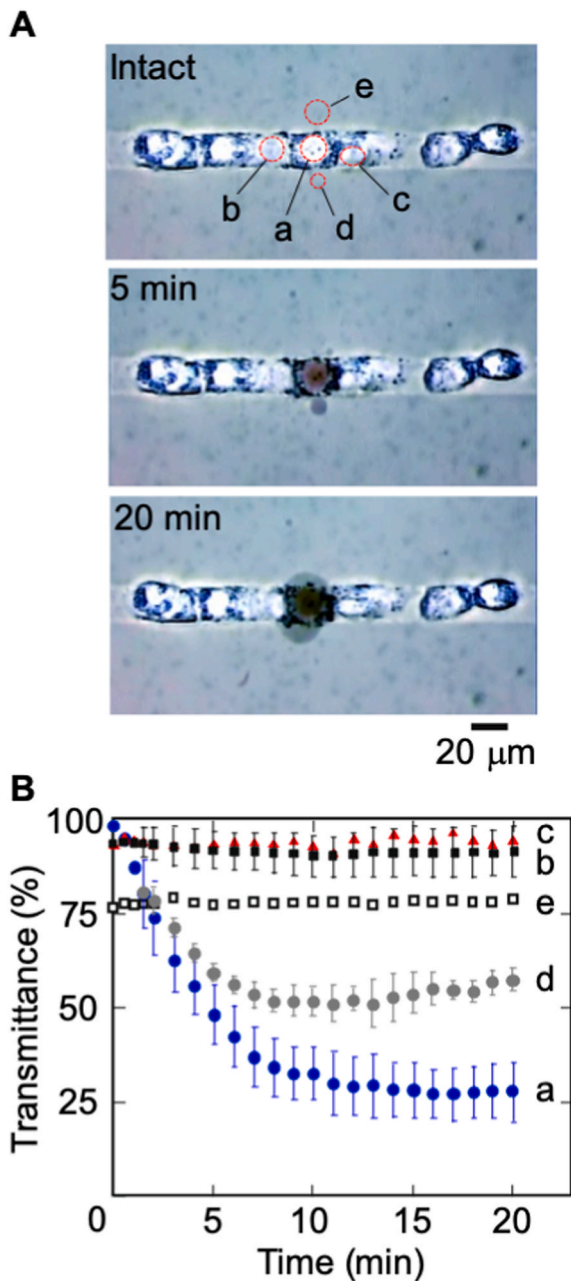
Fig. 1. Trypan blue exclusion test. **A**: bright-field micrographs showing HepG2 before and after laser irradiation. A cell **a** was exposed by NIR fs laser single pulse (50 nJ/pulse, objective NA. 0.5). **B**: Graph showing time-dependent transmittance changes at laser irradiated cell (**a**), adjacent cells (**b** and **c**), bleb (**d**), and buffer (**e**). Reference time zero shows the laser irradiated period. Error bars indicate the standard deviation of intensity observed from pixels. (For interpretation of the references to colour in this figure legend, the reader is referred to the Web version of this article.)

ablated cell underwent apoptosis like cell death while other cells remained intact. Second, we examined a small colony of HepG2 that expressed EGFP in the cytoplasm to assess cell conditions. As shown in Fig. 2B, the cytoplasmic fluorescence of the ablated cell decreased to about 10–15% of the baseline 2 min post ablation. In contrast, the adjacent cells showed negligible change in their cytoplasmic fluorescence.

Having demonstrated the ability of selectively inducing cell death, we proceed to observe any further change occurring on the ablated and adjacent cells. The result displayed in Fig. 3A shows that, while the

trypan blue assay showed that the ablated cell (denoted **a**) exhibited evidence of cell death or injury several min post ablation, it slowly shrank in size and finally detached from the substrate within a few hours post ablation. The time lag between cell death/injury and cell detachment indicates that the binding between receptors on the plasma membrane and ligands of the extracellular matrix may persist for a longer period of time after cell death/injury. The same result also shows that cells (denoted **b**) adjacent to the ablated cell remained intact on the substrate leaving an open space on the substrate (denoted **c**). A careful inspection of the location of the adjacent cells clearly revealed that the neighboring cells tended to migrate towards the open space left by the detached cell (Fig. 3B).

We next examined how the laser energy affected the outcome. In general, the higher the pulse energy, the greater probability of cell detachment (Fig. 3C). Consistently, the duration before cell detachment decreased with the pulse energy (Fig. 3D). Nevertheless, the chance to induce cell death or detachment became rare as the pulse energy decreased to 30 nJ or below.

While the above result shows that the one can manipulate the probability of cell detachment and the temporal duration before detachment by varying laser pulse energy, we found that ablation with a greater pulse energy (single pulse of 200 nJ or 80 MHz pulse train of 70 mW 500 ms) generally ruptured the target cells and triggered death of adjacent cells (shadow, Fig. 3C and D). Accordingly, we suggest that a higher laser energy caused a more severe cell damage, and such the damaged cell might release cytosolic granules, which resembled the feature of necrotic cell death.

As described, the temporal duration required before cell detached became longer when the pulse energy decreased. For instance, it took longer than 5 h for the selected cell to detach for pulse energy approximately 30 nJ (Fig. 3D). Nevertheless, the duration seemed to converge to 54 min $\pm$ 8 min at higher pulse energy (>100 nJ). This result indicates that there seemed to have a cascade of cellular change that eventually led to the breakdown of the binding between the membrane receptor and the ligand of the matrix.

We next evaluate the ability to induce selective cell death *in vivo* by focusing the 80 MHz fs laser to a cardiac cell in the atrial chamber of larval zebrafish. To facilitate precise targeting and selective ablation of cardiomyocytes in the larval heart, we halted the heartbeat temporarily with nifedipine [26]. Furthermore, to facilitate tracking the morphological change and movement of the target and adjacent cells after ablation *in vivo*, we particular employed a fish strain expressing GFP-myosin and mCherry-histone (Fig. 4A).

As shown in Fig. 4A and B, shortly after laser ablation (30 s), the green fluorescence of EGFP-myosin within an area conforming to the dimension of single cell became diminished and completely disappeared (yellow dotted circle); nevertheless, cells away from the ablated remained intact showing no significant change of their fluorescence, indicating that single cardiac cell was ablated. The observation of diminishing EGFP-myosin fluorescence for the ablated cell and the intact fluorescence of the adjacent cells is consistent with results obtained the experiment performed on HepG2 *in vitro* (Fig. 2B). In contrast the drastically decreased EGFP fluorescence, the red fluorescence of mCherry-histone did not change significantly after laser ablation. The finding that the fluorescence of the cytosolic EGFP-myosin disappeared whereas that of the nuclear mCherry-histone remained indicates that the gentle ablation may cause only mild damage to the plasma membrane, and the damaged plasma membrane only allowed permeation of small EGFP-myosin molecules but not large mCherry-histone molecules.

Under such condition, we observed no leak of blood cells from the cardiac chamber. These collective strongly results indicate that the integrity of the cardiac chamber remained intact. Besides, the NIR fs laser ablation caused no discernible sign of damage on the skin and other tissues unless the exposure was prolonged. These results clearly demonstrate the ability to utilize fs laser ablation to selectively damage single cardiac cell of larval zebrafish *in vivo*.
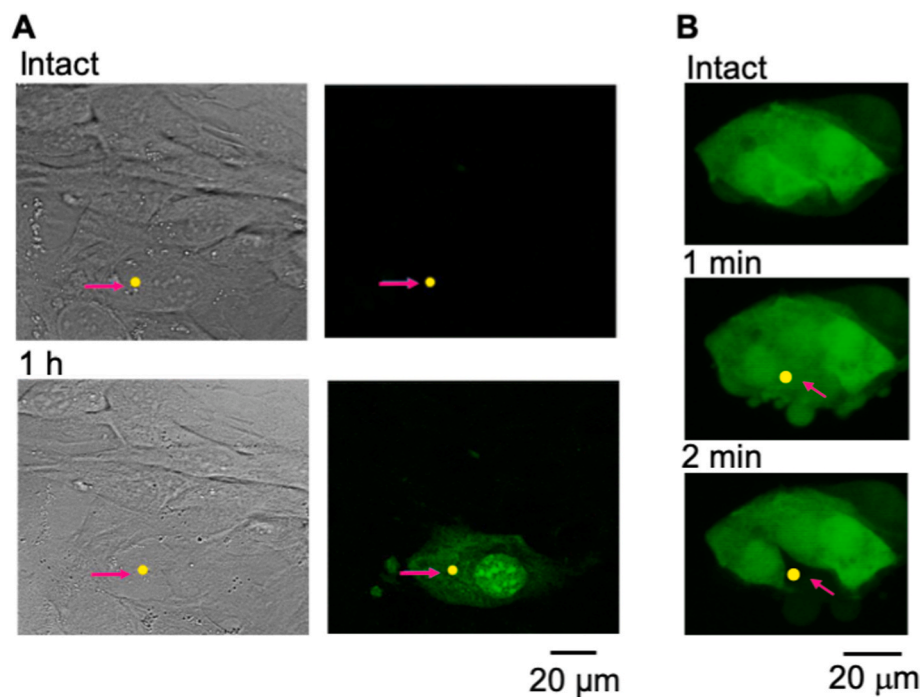
Fig. 2. Apoptosis-like cell death induced by NIR fs laser direct irradiation (80 MHz, 100 ms, 0.875 nJ/pulse, objective NA. 1.2). **A:** Caspase 3/7 activity of a NIR fs laser-irradiated cell and the adjacent cells. Top and bottom sets indicate the pictures before and about after 1 h the NIR fs laser irradiation, respectively. Left and right are blight field and confocal fluorescence images, respectively. The caspase activity shown in right images was observed by a fluorochrome inhibitor FAM-DEVD-FMK. The NIR fs laser was irradiated to the arrowed yellow position. **B:** Fluorescence from EGFP expressed in cytoplasm of a laser-irradiated cell and the adjacent cells. The NIR fs laser was irradiated to the arrowed yellow position. Data **A** and **B** was observed at C2C12 and EGFP expressed HepG2, respectively. (For interpretation of the references to colour in this figure legend, the reader is referred to the Web version of this article.)
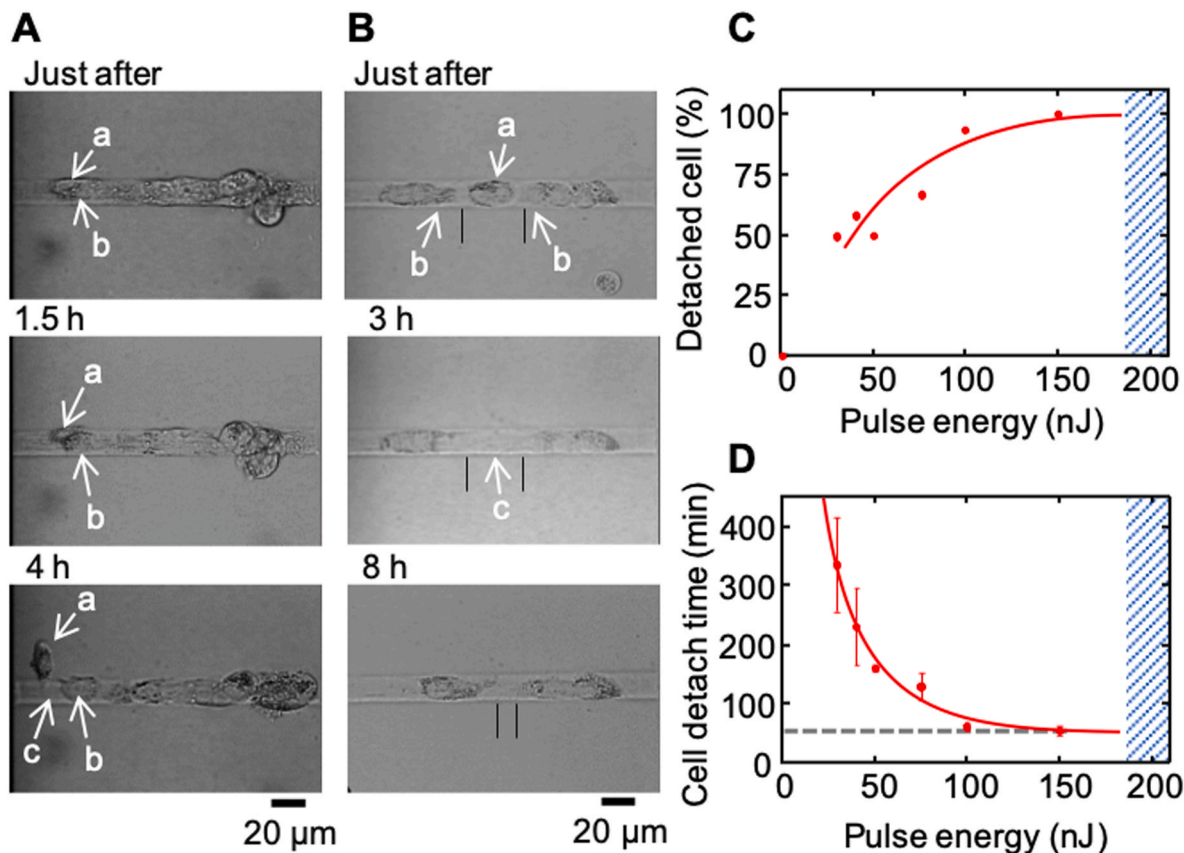

Fig. 3. Cell detachment from the micro-domain after NIR fs laser exposure. **A:** Bright-field micrographs of HepG2 before and after NIR fs laser ablation. A single pulse of NIR fs laser (50 nJ/pulse, objective NA. 0.5) was focused to HepG2 cell indicated by allow **a** in a maintenance medium. **B:** Behavior of adjacent cells after irradiation of the 50 nJ single pulse. Center photograph was observed immediately after the cell detachment. Black lines indicate space between adjacent cells. **C:** Cell detachment probability at different laser pulse energy. **D:** Average cell detachment time of detached cells at different laser pulse energy. The cells not detached after 7.5 h were excluded in this data. Femtosecond laser-induced necrosis-like cell death at laser energy indicated with blue area. (For interpretation of the references to colour in this figure legend, the reader is referred to the Web version of this article.)
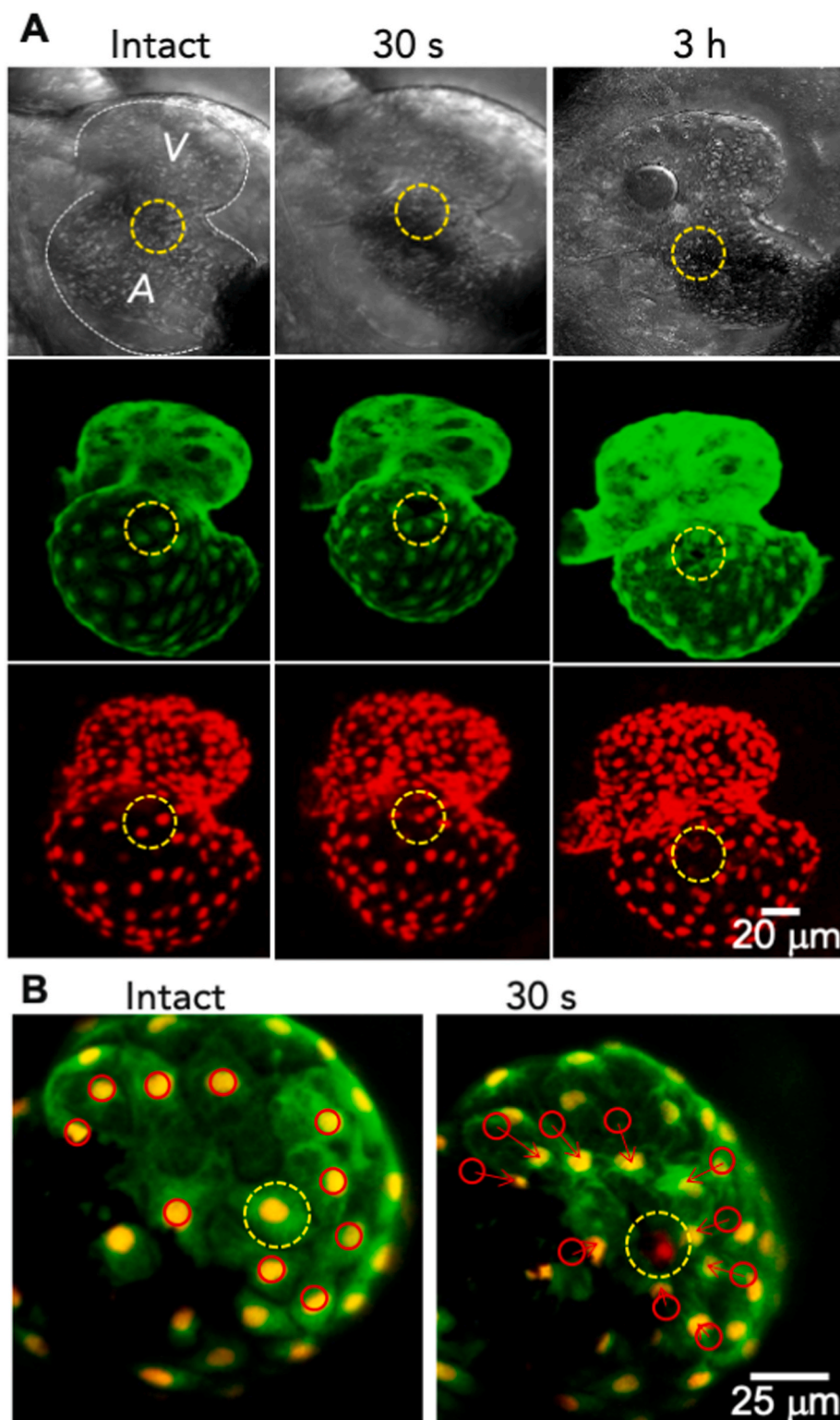
Fig. 4. Closed ablation of zebrafish larvae atrium at target cell level. **A:** Photographs display the same heart obtained before (intact), after about 30 s, and 3 h since the NIR fs laser ablation, respectively (top: bright-field images; middle: EGFP-myosin fluorescence; bottom: mCherry-histone fluorescence). The yellow dotted circle encompasses the region of the cells ablated, in which the NIR fs laser (80 MHz, 100 ms, 0.875 nJ/pulse, objective NA. 1.2) was focused at proximity the center through the larvae skin. Italic letters **A** and **V** indicate the atrium and ventricle, respectively. Particles inside the atrium and ventricle were blood cells (bright-field images). **B:** Overlaid fluorescent images of the atrium of a larva acquired before (left) and after (right) ablation (green: EGFP-myosin; red: mCherry-histone, yellow: overlapped regions of EGFP and mCherry). (For interpretation of the references to colour in this figure legend, the reader is referred to the Web version of this article.)

In addition, our result shows that the domain of disappeared fluorescence appeared to shrink progressively, and the shrinkage of the target cell caused adjacent cells (red circle) to move towards the target cell (red arrows, Fig. 4B). This observation is in good agreement with the result obtained from the *in vitro* experiments (Fig. 3B), and conforms to the morphological characteristics of apoptotic cell death. Taken together, these collective results demonstrate a prospective potential to induce apoptosis of single cardiomyocytes in the myocardium of living

zebrafish by using NIR fs laser ablation.

The NIR fs laser used in this study has a wavelength (800 nm) in a first biological window so the absorption of light by the tissue and the physiological solution is minimum. Along with this, the extremely short pulses (130 fs in duration) indicates that multiphoton ablation occurred almost instantaneously relatively to the slow conduction of heat. Furthermore, the tightly focused laser beam and the high threshold of multiphoton ablation also ensure that the ablation occurred almost

exclusively at the laser focus. Indeed, when the target cell was ablated with femtosecond laser (single pulse of <15 nJ/pulse or pulses of 80 MHz for 0.1 s, 0.875 nJ/pulse), the damage to adjacent cells was negligible.

For comparison, if we employ a CW NIR laser (λ = 1460 nm, 300 mW, duration 3 ms of exposure) to induce injury at the heart of larval zebrafish, it appears to be difficult to confine the damage to single cells [27]. The extended damage area by the CW NIR laser can be explained by the strong absorption of the 1460 nm light by water, which elevates the temperature and causes thermal damage to nearby tissues away from the focal zone. In other words, such limitation would inevitably preclude a precise control of the lesion confining to single cells, and hinder fundamental investigation of cardiac regeneration that may benefit from a selected resection of single cardiomyocytes *in vivo*.

4. Conclusion

In summary, we demonstrate that the utility of NIR fs laser pulses to induce the death and elimination of selected cells *in vivo* and *in vitro*. In both cases utilizing single shot pulse with high pulse energy and 80 MHz repetition pulses, the ablation is induced by non-linear multiphoton absorption processes, so that the NIR fs lasers allow for ablation of target cells in live body. However, it practically depends on transparency of the specimens. The difference between the single shot pulse and high repetition pulse irradiations is presumably in trade-off between heat and mechanical damages of the cell at the laser focal point. Meanwhile, our experimental result showed that neighboring cells have no signs of expected damages. We conclude that the high repetition pulse irradiation is better for in cell ablation applications, because the pulse generation by the fs laser oscillator is easy and stable compared with the single shot pulse generation by regenerative fs laser amplifier. The single shot pulse irradiation with high pulse energy would be valuable in the laser ablation experiments for more complex and thick specimens. Such induction of targeted cell death using NIR fs laser ablation should find broad applications that benefit from precise manipulation at the level of single cells in both *in vivo* and *in vitro*.

CRediT authorship contribution statement

Kazunori Okano: Conceptualization, Supervision, Writing - original draft, conducted the experiments. **Chung-Han Wang:** conducted the experiments. **Zhen-Yi Hong:** conducted the experiments. **Yoichiroh Hosokawa:** Writing - original draft. **Ian Liau:** Conceptualization, designed the work, Supervision, Writing - original draft.

Declaration of competing interest

The authors have declared no conflicts of interest.

Acknowledgements

This study was supported by the Ministry of Education Taiwan under the Aiming Top University program (the MOE ATU project 103W967 to NCTU), and by the Ministry of Science and Technology of Taiwan (MOST-103-2320-B-009-001MY2 to KO and MOST 103-2113-M-009-013-MY3 to IL). The MPC polymer was kindly gifted by NOF Corporation (Tokyo, Japan). We acknowledge the Taiwan Zebrafish Core Facility to support the source of zebrafish.

Appendix A. Supplementary data

Supplementary data to this article can be found online at https://doi.org/10.1016/j.bbrep.2020.100818.

References

[1] C.S. Chen, M. Mrksich, S. Huang, G.M. Whitesides, D.E. Ingber, Geometric control of cell life and death, Science 276 (1997) 1425–1428.
[2] L. Petreanu, A. Alvarez-Buylla, Maturation and death of adult-born olfactory bulb granule neurons: role of olfaction, J. Neurosci. 22 (2002) 6106–6113.
[3] N. Kaneko, O. Marín, M. Koike, Y. Hirota, Y. Uchiyama, J.Y. Wu, Q. Lu, M. Tessier-Lavigne, A. Alvarez-Buylla, H. Okano, J.L.R. Rubenstein, K. Sawamoto, New neurons clear the path of astrocytic processes for their rapid migration in the adult brain, Neuron 67 (2010) 213–223.
[4] J. Itou, I. Oishi, H. Kawakami, T.J. Glass, J. Richter, A. Johnson, T.C. Lund, Y. Kawakami, Migration of cardiomyocytes is essential for heart regeneration in zebrafish, Development 139 (2012) 4133–4142.
[5] P. Friedl, D. Gilmour, Collective cell migration in morphogenesis regeneration and cancer, Nat. Rev. Mol. Cell Biol. 10 (2009) 445–457.
[6] N. Kapoor, W. Liang, E. Marbán, H.C. Cho, Direct conversion of quiescent cardiomyocytes to pacemaker cells by expression of Tbx18, Nat. Biotechnol. 31 (2013) 54–62.
[7] M. Kashii, Y. Hosokawa, H. Kitano, H. Adachi, Y. Mori, K. Takano, H. Matsumura, T. Inoue, S. Murakami, H. Sugamoto, H. Yoshikawa, T. Sasaki, H. Masuhara, Femtosecond laser-induced cleaving of protein crystal in water solution, App. Surf. Sci. 253 (2007) 6447–6450.
[8] A. Uchugonova, M. Lessel, S. Nietzsche, C. Zeitz, K. Jacobs, C. Lemke, K. König, Nanosurgery of cells and chromosomes using near-infrared twelve-femtosecond laser pulses, J. Biomed. Opt. 17 (2012) 101502.
[9] M.F. Yanik, H. Cinar, H.N. Cinar, A.D. Chisholm, Y. Jin, A. Ben-Yakar, Functional regeneration after laser axotomy, Nature 432 (2004) 822.
[10] U.K. Tirlapur, K. König, Femtosecond near-infrared laser pulses as a versatile non-invasive tool for intra-tissue nanoprocessing in plants without compromising viability, Plant J. 31 (2002) 365–374.
[11] W. Watanabe, S. Matsunaga, T. Shimada, T. Higashi, K. Fukui, K. Itoh, Femtosecond laser disruption of mitochondria in living cells, Med. Laser Appl. 20 (2005) 185–191.
[12] A. Uchugonova, A. Isemann, E. Gorjup, G. Tempea, R. Bückle, W. Watanabe, K. König, Optical knock out of stem cells with extremely ultrashort femtosecond laser pulses, J. Biophoton 1 (2008) 463–469.
[13] K. König, O. Krauss, I. Riemann, Intratissue surgery with 80 MHz nanojoule femtosecond laser pulses in the near infrared, Opt. Exp. 10 (2002) 171–176.
[14] K. Okano, D. Yu, A. Matsui, Y. Maezawa, Y. Hosokawa, A. Kira, M. Matsubara, I. Liau, H. Tsubokawa, H. Masuhara, Induction of cell–cell connections by using *in situ* laser lithography on a perfluoroalkyl-coated cultivation platform, ChemBioChem 12 (2011) 795–801.
[15] H. Yamamoto, K. Okano, T. Demura, Y. Hosokawa, H. Masuhara, T. Tanii, S. Nakamura, In-situ guidance of individual neuronal processes by wet femtosecond-laser processing of self-assembled monolayers, Appl. Phys. Lett. 99 (2011) 163701.
[16] K. Okano, H.-Y. Hsu, Y.-K. Li, H. Masuhara, *In situ* patterning and controlling living cells by using femtosecond laser, J. Photochem. Photobiol. C 28 (2016) 1–28.
[17] Y.-E. Kuo, C.-C. Wu, H. Hosokawa, Y. Maezawa, K. Okano, H. Masuhara, F.-J. Kao, Local stimulation of cultured myocyte cells by femtosecond laser-induced stress wave, Appl. Phys. A 101 (2010) 597–600.
[18] U.K. Tirlapur, K. König, Targeted transfection by femtosecond laser, Nature 418 (2002) 290–291.
[19] D. Stevenson, B. Agate, X. Tsampoula, P. Fisher, C.T.A. Brown, W. Sibbett, A. Riches, F. Gunn-Moore, K. Dholakia, Femtosecond optical transfection of cells: viability and efficiency, Opt. Exp. 14 (2006) 7125–7133.
[20] Y. Hosokawa, S. Iguchi, R. Yasukuni, Y. Hiraki, C. Shukunami, H. Masuhara, Gene delivery process in a single animal cell after femtosecond laser microinjection, Appl. Surf. Sci. 255 (2009) 9880–9884.
[21] T. Maeno, T. Uzawa, I. Kono, K. Okano, T. Iino, K. Fukita, Y. Oshikawa, T. Ogawa, O. Iwata, T. Ito, K. Suzuki, K. Goda, Y. Hosokawa, Targeted delivery of fluorogenic peptide aptamers into live microalgae by femtosecond laser photoporation at single-cell resolution, Sci. Rep. 8 (2018) 8271.
[22] U.K. Tirlapur, K. König, C. Peuckert, R. Krieg, K.-J. Halbhuber, Femtosecond near-infrared laser pulses elicit generation of reactive oxygen species in mammalian cells leading to apoptosis-like death, Exp. Cell Res. 263 (2001) 88–97.
[23] J. Yoon, S.-w. Ryu, S. Lee, C. Choi, Cytosolic irradiation of femtosecond laser induces mitochondria-dependent apoptosis-like cell death via intrinsic reactive oxygen cascades, Sci. Rep. 5 (2015) 8231.
[24] W. Strober, Trypan blue exclusion test of cell viability, Curr. Protoc. Im. 21 (1997). A-3B1–A-3B2.
[25] K. Okano, A. Matsui, Y. Maezawa, P.-Y. Hee, M. Matsubara, H. Yamamoto, Y. Hosokawa, H. Tsubokawa, Y.-K. Li, F.-J. Kao, H. Masuhara, *In situ* laser micropatterning of proteins for dynamically arranging living cells, Lab Chip 13 (2013) 4078–4086.
[26] U. Langheinrich, G. Vacun, T. Wagner, Zebrafish embryos express an orthologue of HERG and are sensitive toward a range of QT-prolonging drugs inducing severe arrhythmia, Toxicol. Appl. Pharmacol. 193 (2003) 370–382.
[27] G. Matrone, J.M. Taylor, K.S. Wilson, J. Baily, G.D. Love, J.M. Girkin, J.J. Mullins, C.S. Tucker, M.A. Denvir, Laser-targeted ablation of the zebrafish embryonic ventricle: a novel model of cardiac injury and repair, Int. J. Cardiol. 168 (2013) 3913–3919.